Front. Energy Power Eng. China 2010, 4(4): 443–458
DOI 10.1007/s11708-010-0127-5

FEATURE ARTICLE

T.S. Zhao, Y.S. Li, S.Y. Shen

Anion-exchange membrane direct ethanol fuel cells: Status and perspective

Abstract Direct ethanol fuel cells (DEFCs) are a promising carbon-neutral and sustainable power source for portable, mobile, and stationary applications. However, conventional DEFCs that use acid proton-exchange membranes (typically Nafion type) and platinum-based catalysts exhibit low performance (i.e., the state-of-the-art peak power density is 79.5 mW/cm^2 at 90°C). Anion-exchange membrane (AEM) DEFCs that use low-cost AEM and non-platinum catalysts have recently been demonstrated to yield a much better performance (i.e., the state-of-the-art peak power density is 160 mW/cm^2 at 80°C). This paper provides a comprehensive review of past research on the development of AEM DEFCs, including the aspects of catalysts, AEMs, and single-cell design and performance. Current and future research challenges are identified along with potential strategies to overcome them.

Keywords fuel cell, direct ethanol fuel cells, anion-exchange membrane, ethanol oxidation reaction, oxygen reduction reaction, cell performance

1 Introduction

The growing global energy demand and the large-scale use of CO_2-emitting fossil fuels pose a great threat to our already damaged planet. Hence, developing renewable energy sources at a global scale is urgent for the sustainable development of our society. Fuel cells have been identified as one of the most promising technologies for the clean energy industry of the future. Fuel cells convert the chemical energy stored in fuel, such as hydrogen, into electrical energy output through electrochemical reactions. Currently, hydrogen is commonly used as fuel to energize fuel cells, particularly proton exchange membrane fuel cells (PEMFCs). However, the production of pure hydrogen is currently expensive, and there are tremendous challenges in transporting, storing, and handling gaseous hydrogen. For this reason, liquid hydrogen-rich alcohol fuels, which have a much higher energy density and are easier to transport, store, and handle, have become an attractive alternative to hydrogen for direct oxidation fuel cells. Among various alcohol fuels, methanol has been considered the most promising primarily because it has the simplest molecular structure without carbon bonds and is thus easier to oxidize than other alcohol fuels. Hence, direct methanol fuel cells (DMFCs) have been extensively studied over the past few decades [1–5]. However, in addition to the low performance problem associated with sluggish anode reaction kinetics [6–8] and methanol crossover [9–11] in DMFCs, the inherent disadvantage of methanol is its toxicity, which makes the fuel unsustainable and unsafe for consumer use. In contrast, ethanol is much less toxic than methanol; it has higher energy density (8.0 kW·h/kg) than methanol (6.1 kW·h/kg) and can be produced in great quantity from biomass through a fermentation process from renewable resources, such as sugar cane, wheat, corn, or even straw. More importantly, the CO_2 emitted during the energy production process from ethanol can be soaked up by growing plants from which the fuel is produced. Hence, ethanol is a sustainable, carbon-neutral fuel source, and direct ethanol fuel cells (DEFCs) are clearly the best choice for producing sustainable energy in the future.

Past research on the development of DEFCs has focused mainly on the so-called PEM DEFCs that use PEM as the electrolyte, a Pt-based catalyst on the anode, and a pure Pt catalyst on the cathode [12–18]. The advantage of PEM DEFCs is that the entire system setup and all the components can be the same as those in current DMFC technologies that also use PEMs. With regard to the catalysts in PEM DEFCs, previous studies have demonstrated that the catalytic activity of PtRu- and PtSn-based

Received August 3, 2010; accepted September 14, 2010

T.S. Zhao (✉), Y.S. Li, S.Y. Shen
Department of Mechanical Engineering, The Hong Kong University of Science and Technology, Kowloon, Hong Kong SAR, China
E-mail: metzhao@ust.hk

catalysts, both binary and ternary, on the ethanol oxidation reaction (EOR) in an acid media is higher than that of pure Pt catalysts due to the bifunctional mechanism and electronic effect [12]. By combining Pt with Ru, the oxidation of strongly bound adsorbed intermediates is enhanced to give a relatively high yield of CO_2 [13]. Recently, Basu et al. [14] systematically studied the effect of operating parameters on the performance of a PEM DEFC with PtRu as the anode catalyst and showed a peak power density of 10.3 mW/cm^2 at 90°C. Zhou et al. [15] showed that the sequence of catalytic activity for the EOR is PtSn > PtRu > PtW > PtPd > Pt, indicating that PtSn-based catalysts are better than the PtRu based, which is the state-of-the-art anode catalyst for DMFCs. However, the catalytic activity of PtSn was found to vary with the preparation method [16] and the content of both alloyed and non-alloyed Sn [17]. Léger et al. [18] synthesized PtSn catalysts and determined the optimum composition of Sn to be in the range of 10%–20% (atom fraction). These catalysts achieved a peak power density of about 28 mW/cm^2 at 90°C.

In summary, although tremendous efforts have been expended on developing EOR catalysts for PEM DEFCs, the performance of PEM DEFCs remains low even at relatively high operating temperatures, such as at 90°C. The low performance of this type of fuel cell is mainly because the kinetics of the EOR in acid media is slow, leading to a large activation loss. Another critical obstacle that limits the wide application of PEM DEFCs is the cost of the system, not only because a considerable amount of Pt-based catalysts at both the anode and cathode is required but also because acid electrolyte membranes (typically Nafion) are expensive.

Unlike in acid media, the kinetics of both the EOR and oxygen reduction reaction (ORR) in alkaline media is much faster and allows the use of non-precious metal catalysts to reduce the cost of the fuel cell. Similar to the use of PEM in acid fuel cells, the use of an anion-exchange membrane (AEM) instead of a caustic alkaline liquid electrolyte in an alkaline fuel cell can solve carbonation and other related problems, such as electrolyte leakage and precipitation of carbonate salts. AEM DEFCs have recently attracted increasing attention due to the reasons cited above [19–26]. This article provides a comprehensive review of the past research on the development of AEM DEFCs, including the aspects of catalysts, AEMs, and single cell systems. Current and future research challenges are identified along with the potential strategies to overcome them. The remainder of this paper is organized as follows: Section 2 describes the general setup and working principle of the AEM DEFC; Sections 3–6 review the current status of this type of fuel cell, including AEMs, catalysts for both the EOR and ORR, and the single-cell design and performance. Finally, a summary and outlook are given in Section 7.

2 General setup and working principle

Figure 1 illustrates a typical liquid-feed AEM DEFC setup that consists of a membrane electrode assembly (MEA) sandwiched by an anode and a cathode bipolar plate. The MEA, which is regarded as an integrated multi-layered structure, is composed sequentially of an anode diffusion layer (DL), an anode catalyst layer (CL), an AEM, a cathode CL, and a cathode DL. The function of the membrane is to conduct hydroxyl ions from the cathode to the anode and act as a separator between the anode and cathode electrodes. Typically, quaternized hydrocarbon AEMs (e.g. A201 by Tokuyama) are used in AEM DEFCs [27]. The CLs at both the anode and cathode are usually comprised of catalysts mixed with ionomer to provide triple-phase boundaries for the EOR and ORR. The DLs consist of two layers, a backing layer (BL) made of carbon cloth or carbon paper, and a micro-porous layer (MPL) composed of a hydrophobic polymer and carbon powder. The function of each DL is to provide support for the corresponding CL, to distribute evenly the reactants over the CL, and to conduct electricity to the current-collector. On the anode, the ethanol solution flowing into the anode flow field is transported through the anode DL to the anode CL, where ethanol is oxidized to generate electrons, water, and CO_2 according to

$$CH_3CH_2OH + 12OH^- \rightarrow 2CO_2 + 9H_2O + 12e^- \quad (1)$$

The water in ethanol solution, along with that produced from the EOR, diffuses through the membrane to the cathode CL, while the electrons travel through an external circuit to the cathode. On the cathode, the oxygen/air provided by the cathode flow field is transported through the cathode DL to the cathode CL, where the oxygen reacts with water from the anode to produce hydroxide ions according to

$$3O_2 + 6H_2O + 12e^- \rightarrow 12OH^- \quad (2)$$

Subsequently, the generated hydroxide ions are conducted to the anode for the EOR, as indicated by Eq. (1). The ideal overall reaction in the AEM DEFC is

$$CH_3CH_2OH + 3O_2 \rightarrow 2CO_2 + 3H_2O \quad (3)$$

However, it should be noted that with the state-of-the-art anode catalysts, the complete oxidation of ethanol expressed by Eq. (1) is not achieved. The main product of the reaction is acetic acid rather than CO_2 [19], i.e.,

$$CH_3CH_2OH + 4OH^- \rightarrow CH_3COOH + 3H_2O + 4e^- \quad (4)$$

In the present AEM DEFC system, to obtain appreciable kinetics of the EOR and ionic conductivity of AEMs, additional alkali needs to be added to the ethanol solution. The produced acetic acid reacts with hydroxyl ions to form acetate ions, i.e.,

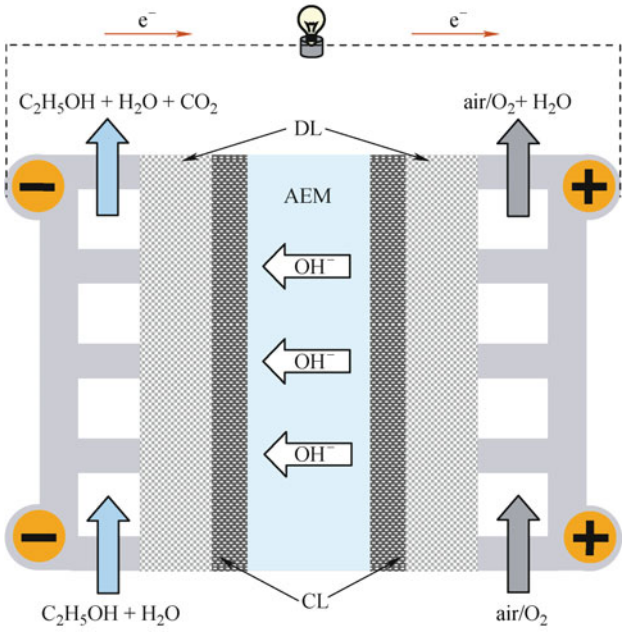

Fig. 1 Schematic of a liquid-feed alkaline membrane-based direct ethanol fuel cell

$$CH_3COOH + OH^- \rightarrow CH_3COO^- + H_2O \quad (5)$$

Hence, the actual overall reaction in the AEM DEFC with the state-of-the-art catalysts is

$$CH_3CH_2OH + O_2 + OH^- \rightarrow CH_3COO^- + 2H_2O \quad (6)$$

In the following, we review the recent developments of the key components, including AEMs, electro-catalysts for the EOR and ORR, as well as the system design and cell performance.

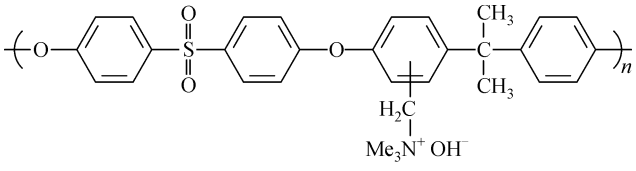

Fig. 2 Structure unit of the quaternary ammonium polysulphone membrane [37]

3 Membranes

Anion-exchange membranes are the enabler of the concept of AEM DEFCs. In terms of the ionic conduction mode within the polymer structure, anion-exchange membranes can be classified into two types: the polyelectrolyte membrane and the alkali-doped polymer membrane [28]. The development of these two types of anion-exchange membrane, including its composition, ionic conductivity, ethanol permeability, and thermal and chemical stability, is described below.

3.1 Polyelectrolyte membranes

The polyelectrolyte membrane is essentially an ionomer. As shown in Fig. 2, the ionic function groups (typically quaternary ammonium) are grafted on the skeleton of the polymer backbone, and the mobile hydroxyl ions are associated to each ionic function groups to maintain membrane electro-neutrality [28]. A typical commercial product of polyelectrolyte membranes is the A201 membranes by Tokuyama; it is composed of quaternary ammonium groups grafted on a hydrocarbon polymer backbone [27]. To date, a number of polymer materials as the backbone have been investigated [29–47], including chitosan [29], poly(2,6-dimethyl-1,4-phenylene oxide) (PPO) [30], poly(vinylbenzyl chloride) (PVBCl) [31], poly(tetrafluoroetheneco-hexafluoropropylene) (FEP) [32], and poly(ethylene-co-tetrafluoroethylene) (ETFE) [33–35]. Two kinds of side chains have also been extensively studied: the phenyltrimethylammonium and benzyltrimethylammonium groups.

Ionic conductivity is one of the most important membrane properties. Stoica et al. [48] synthesized a

poly(epichlorydrin-allyl glycidyl ether) copolymer-based alkaline membrane, where anion conducting networks are obtained by incorporating two cyclic diamines called 1,4-diazabicyclo-[2.2.2]-octane (DABCO) and 1-azabicyclo-[2.2.2]-octane (Quinuclidine). The ionic conductivity of this membrane was as high as 2.5×10^{-3} S/cm at 20°C and 1.3×10^{-2} S/cm at 60°C (Note that the typical ionic conductivity of Nafion membranes is around 10^{-1} S/cm at 60°C). Xu et al. [49] prepared and characterized chloroacetylated poly (2,6-dimethyl-1,4-phenyleneoxide) (CPPO) and bromomethylated poly (2,6-dimethyl-1,4-phenylene oxide) (BPPO) blend alkaline membranes. The ionic conductivity of this blend membrane with 20% (mass fraction) CPPO was 3.2×10^{-2} S/cm at 25°C. Varcoe et al. [25,50] reported an ETFE-based radiation-grafted membrane with an ionic conductivity of around 3×10^{-2} S/cm at room temperature, which increased to 6×10^{-2} S/cm when fully hydrated at 60°C. To improve ionic conductivity, Agel et al. [28] studied the influence of the KOH concentration on ionic conductivity. The results indicated that ionic conductivity was first increased and then decreased with the KOH concentration and that the optimal KOH concentration with ionic conductivity of 4×10^{-2} S/cm was 3.5 M at 25°C. Yanagi et al. [51,52] reported that the OH^- in the A201 membrane could be changed to CO_3^{2-} or HCO_3^- within 30 min due to the absorption of CO_2. However, further investigations revealed that a self-purging function in the AEMs, by which the CO_3^{2-} or HCO_3^- in the A201 membrane could change to OH^- under the discharging process that suppressed the neutralization of alkaline AEMs and ionomer [27,52–54].

The quaternary ammonium group-based AEMs have particularly low thermal and chemical stability. There are mainly two degradation mechanisms, as shown in Fig. 3 [21,25]: direct nucleophilic displacement and Hoffmann elimination reaction. The ionic conductivity of phenyltrimethylammonium group-based AEMs decreases through direct nucleophilic displacement mechanism, whereas for benzyltrimethylammonium group-based AEMs containing β-hydrogen atoms, both mechanisms work. However, Los Alamos National Laboratory [55] reported that although it contained the β-hydrogen atom, benzyltrimethylammonium hydroxides exhibited much better stability than phenyltrimethylammonium hydroxides. Yanagi et al. [27] reported the durability of the commercial A201 membrane in water and methanol at 80°C and showed that the ion-exchange capacity (IEC) was stable for 2300 h. In addition, the organic-inorganic hybrid membranes [56–60] that introduced an inorganic component into the organic polymer matrix, enhanced the thermal and chemical stability of the membranes [20]. The thermal degradation temperature in air was in the range of 250°C–300°C, and the durability time in Fenton's reagent could reach 12 h [60].

With respect to alcohol permeability through membranes, Varcoe et al. [61] compared the permeability of methanol, ethanol, and ethylene glycol among the ETFE-based radiation-grafted AEM, a cross-linked quaternary ammonium-type AEM, and Nafion-115 PEM as shown in Fig. 4. The alcohol in AEM showed lower permeability than that in PEM, and ethanol had the lowest permeability in AEM. Yang et al. [43] investigated the permeability of methanol, ethanol, and 2-propanol based on the PVA/TiO_2 hybrid membrane and showed that the permeability of the PVA/TiO_2 hybrid membrane was in the order of 10^{-7} to 10^{-8} cm^2/s, much lower than that of the Nafion membrane in the order of 10^{-6} cm^2/s.

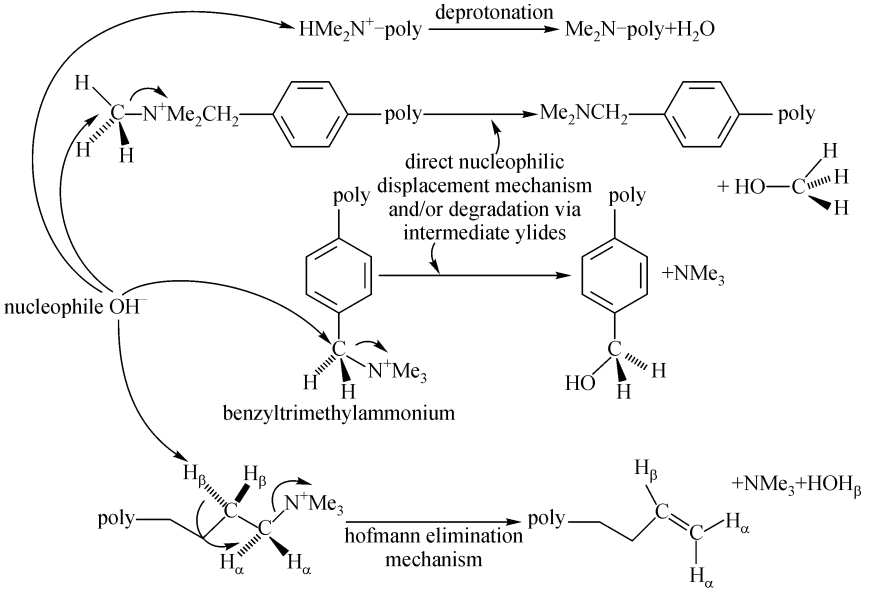

Fig. 3 Principal hydroxide anion-induced alkaline anion-exchange membrane chemical headgroup degradation pathways [25]

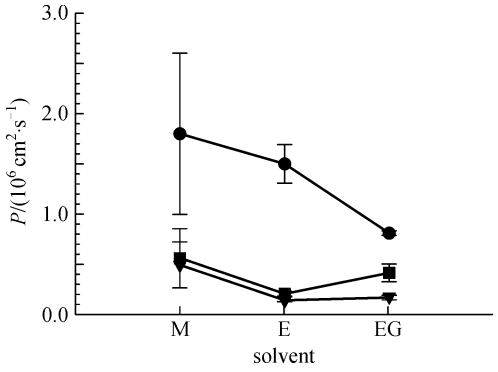

Fig. 4 Solvent permeability of ETFE-AEM (■), Cross-linked AEM (▼) and Nafion-115 (●) at room temperature. M = methanol, E = ethanol and EG = ethylene glycol [61]

3.2 Alkali-doped polymer membranes

The alkali-doped polymer membrane, as shown in Fig. 5, is composed of electronegative heteroatoms (typically nitrogen) that interact with the cations of alkali by a donor-acceptor link. The principle of ionic conduction in the alkali-doped polymer membrane is based on the heteroatom-cation interactions and the mobility of amorphous polymer chains [28]. A typical sample for alkali-doped polymer membranes is the KOH-doped polybenzimidazole (PBI) membrane [27]. Savadogo et al. [62] reported that the ionic conductivity of KOH-doped PBI membrane is in the range of $5\times10^{-5}-10^{-1}$ S/cm; the highest ionic conductivity of 9×10^{-2} S/cm is achieved at 25°C. The study by Fu et al. [63] indicated that the ionic conductivity of the KOH-doped PVA membrane first increased and then decreased with the KOH concentration, and this was because the high KOH concentration induced weak ionic mobility, such as formed ion-pairs or increased viscosity, thereby reducing ionic conductivity. In addition, the KOH-doped PVA membrane exhibited excellent thermal and chemical stability to high KOH concentration (10 M) at a high temperature of 120°C. The stability of the alkali-doped polymer membranes is superior to the quaternized polyelectrolyte membranes. Leykin et al. [64] showed that the ethanol permeability of KOH-doped PBI membrane first increased and then decreased with the increase in the KOH concentration. Ethanol permeability through KOH-doped PBI membrane was 6.5×10^{-7} cm^2/s, which is much lower than that of Nafion membrane. The reason is that Nafion membranes swelled more significantly than KOH-doped PBI membranes. The less expanded space among PBI backbones than that of the Nafion probably resulted in the lower ethanol permeability in KOH-doped PBI membrane [65].

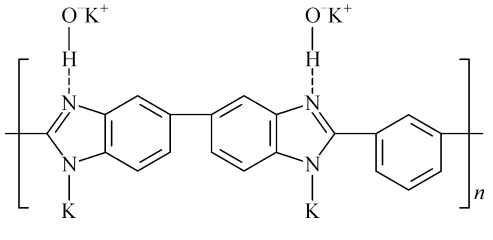

Fig. 5 Structure unit of the alkali-doped PBI membrane [65]

In summary, we have discussed the two types of anion-exchange membranes: the polyelectrolyte membrane and alkali-doped polymer membrane. The ionic conductivity and the thermal and chemical stability of both types of membranes are still low. Hence, significant work is required to improve membrane performance. Research is also needed in the aspects of characterizations of anion-exchange membrane properties, including water uptake, ethanol permeability, water diffusivity, and electro-osmotic drag coefficient [66–71].

4 Ethanol oxidation electrocatalysis

4.1 Pd-based catalysts

Platinum is the best known material for the dissociative adsorption of small organic molecules at low temperatures, and PtRu/C and PtSn/C have been widely accepted as the most effective catalysts for EOR in acid media [72,73]. However, because Pt is scarce and expensive, palladium has recently attracted attention as an alternative catalyst for the alcohol oxidation reaction, especially for EOR in alkaline media. Unlike the Pt catalyst, the Pd catalyst shows better tolerance to the CO-containing intermediates. Moreover, Pd is 50 times more abundant than Pt on earth. To enhance the performance of Pd for the EOR in alkaline media, many studies have reported on nanosized Pd catalysts. Hou et al. [74] prepared Pd spherical nanoparticles, multitwinned particles, and spherical spongelike particles (SSPs) in the presence of different surfactants or polymers. Among which, the Pd SSPs showed the highest catalytic activity and the best stability for EOR in alkaline media due to its uniquely interconnected structure. Wang et al. [75] fabricated a nanoporous Pd (NPPd) catalyst with a ligament size of 3–6 nm by chemically dealloying binary Al-Pd alloys in alkaline solution. The nanoporous Pd catalyst exhibited an electrochemical active surface area of 23 m^2/g, and the mass catalytic activity for EOR in alkaline media could reach 148 mA/mg. Pd nanowires with a length of a few tens of nanometers were synthesized by Remita et al. [76] using hexagonal mesophases as templates. Pd nanowires exhibited both very good catalytic activity and high stability for EOR in alkaline media.

Shen et al. [77, 78] prepared a series of metal oxides (i.e., CeO_2, NiO, Co_3O_4, and Mn_3O_4) and promoted Pd catalysts using these metal oxides coated with carbon powder by intermittent microwave heating method. These catalysts exhibited higher activity and better stability than

both Pt and Pd catalysts for the EOR in alkaline media. Among the different metal oxides, the Pd-NiO/C-modified electrode with a 6∶1 weight ratio (Pd loading: 0.30 mg/cm^2) was found to give the highest performance: its peak current density was 74 mA/cm^2, and the onset potential was −0.07 V. Chu et al. [79] studied EOR on carbon nanotube-supported and In_2O_3-promoted Pd catalysts in alkaline media prepared using chemical reduction and hydrothermal reaction process. The Pd-In_2O_3/CNTs modified electrode with a 10∶3 weight ratio (Pd loading: 0.20 mg/cm^2) showed the highest activity. The peak current density was 61 mA/cm^2, and the onset potential was −0.262 V. The improvement due to the incorporation of metal oxides was attributed to the fact that the metal oxides could function as active sites for the formation of oxygen-containing species that would help remove the adsorbed ethoxi species according to the bifunctional mechanism as Ru in the PtRu catalyst [77–79].

Attempts have also been made to combine Pd with another metal, M (M = Au, Sn, Ag, Ru, Cu, Ni and Pb), to improve catalytic activity for the EOR in alkaline media. He et al. [80] compared the catalytic activity of Pd_4Au/C and $Pd_{2.5}Sn$/C catalysts for the EOR in alkaline media with that of the Pt/C catalyst, and the results suggested that although the kinetics was somewhat more sluggish on both $Pd_{2.5}Sn$/C and Pd_4Au/C catalysts than on Pt/C, the Pd-based alloy catalysts had higher tolerance to surface poisoning. The Pd_4Au/C catalyst displayed the best catalytic activity for the EOR in alkaline media. The EOR in alkaline media on the Pd-decorated Au catalysts with an Au core/Pd shell (Pd@Au) structure was studied, and higher stability was obtained for the Pd@Au/C catalysts, according to the results given by Zhao et al. [81], Remita et al. [82], and Li et al. [83]. Wang et al. [84, 85] prepared carbon supported Pd-M (M = Pb and Ag) catalysts with different Pd/M atomic ratios using the co-reduction method. The X-ray diffraction characterizations confirmed alloy formation between Pd and M. Electrochemical testing results demonstrated that for the PdPb/C catalysts, the Pd_4Pb_1/C catalyst gave the highest catalytic activity for the EOR in alkaline media whereas it was Pd_1Ag_1/C for the PdAg/C catalysts. The promoting effect of Pb or Ag addition to Pd for EOR in alkaline media can be explained by a bi-functional mechanism and a d-band theory. With the addition of Pb or Ag to Pd, the d-band center of Pd can be shifted up and can result in more OH_{ads} groups being adsorbed onto the catalyst surface, assisting in the removal of the adsorbed ethoxi species. Chen et al. [86] demonstrated that the incorporation of Ru into Pd with a 1∶1 atomic ratio could greatly improve its catalytic activity for the EOR in alkaline media with the onset potential shifting negatively by about 150 mV. Jou et al. [87] electrodeposited PdCu alloy on indium tin oxide (ITO) and compared its catalytic activity for EOR in alkaline media with that of Pd/ITO. The Pd_9Cu/ITO catalyst possessed an onset potential of −0.55 V, a peak current density of 82 mA/cm^2, and a ratio of 4 of forward peak current density to backward peak current density, whereas the peak current density is −0.4V, 17 mA/cm^2 and the ratio is 1 for the Pd/ITO catalyst. Singh et al. [88] investigated the catalytic activity of binary and ternary composite films of Pd, Ni, and MWCNTs for EOR in alkaline media. Zhao et al. [89] and Ma et al. [90] studied the EOR on the PdNi catalysts in alkaline media prepared by the electrodeposition and simultaneous reduction method, respectively. According to the analysis by Zhao et al. [89], the Ni species included metallic Ni, NiO, $Ni(OH)_2$, and NiOOH, and the main component of the Ni species, $Ni(OH)_2$, and NiOOH could chiefly account for the great promotion of EOR on Pd in alkaline media through the reversible redox:

$$Ni(OH)_2 + OH^- \Longleftrightarrow NiOOH + H_2O + e^- \qquad (7)$$

Furthermore, nickel hydroxides can facilitate the oxidation of H_{ads} on Pd surface via the hydrogen spillover effect. The uniform distribution of Ni species around Pd prepared using the simultaneous reduction method can also contribute to the catalytic activity. Bianchini et al. [91] deposited very small (i.e., 0.5–1 nm), highly dispersed, and highly crystalline Pd clusters as well as single Pd sites, likely stabilized by the interaction with oxygen atoms from Ni-O moieties, on the Ni-Zn and Ni-Zn-P alloys supported on Vulcan XC-72 by the spontaneous deposition of Pd through redox transmetalation with Pd^{IV} salts.

The promoting effect of different supporting materials on the EOR in alkaline media on the Pd-based catalysts was studied extensively, including the commonly used carbon black, carbon nanotubes [92], carbon microspheres [93], coin-like hollow carbon [94], tungsten carbide nanocrystals/nanotubes [95, 96], carbonized porous anodic alumina [97], carbonized TiO2 nanotubes [98], activated carbon nanofibers [92], zeolite graphite [99], and conducting polymers (PEDOT, PANI and PA6) [100–102].

4.2 Oxidation mechanism and products

Unlike the methanol oxidation reaction, EOR undergoes both parallel and consecutive oxidation reactions, resulting in more complicated adsorbed intermediates and byproducts. Most importantly, the complete oxidation of ethanol to CO_2 requires the cleavage of C–C bond, which is between two atoms with little electron affinity or ionization energy, making it difficult to break the C-C bond at low temperatures [103,104]. Recently, both mechanistic study and product analysis for EOR on the Pd catalyst in alkaline media have been conducted [105,106]. Zhao et al. [105] studied the mechanism of EOR on the Pd catalyst using the cyclic voltammetry method and suggested that the dissociative adsorption of ethanol was rather quick and that the rate-determining step was the removal of adsorbed ethoxi species by the OH_{ads} groups on Pd. At higher potentials, the kinetics was affected by both the adsorption

of OH_{ads} groups and the formation of the inactive oxide layer on Pd. The theoretical analysis conducted by Cui et al. [106] using the first-principles method based on the density functional theory showed that EOR on the Pd catalyst in acid media was difficult due to the lack of OH_{ads} groups; however, in alkaline media, both ethanol and sufficient OH_{ads} groups could adsorbed on the Pd catalyst, leading to continuous ethanol oxidation. In-situ Fourier transform infrared spectroscopy combined with cyclic voltammetry was employed to examine the online products of EOR on the Pd catalyst in alkaline media [107,108]. Fang et al. [107] studied the effect of pH value of fuel solution on the products and found that the main oxidation product was acetic acid when the OH^- ions concentration was higher than 0.5 M; CO_2 formation was observed only at a pH value equal or smaller than 13. Zhou et al. [108] gave a quantitative analysis of the selectivity for ethanol oxidation to CO_2 at a pH value of 13, and less than 2.5% was observed in the potential region from -0.6 to 0 V. Bambagioni et al. [109] used the $^{13}C\{^1H\}$ NMR spectroscopy to observe anode exhaust from a passive AEM DEFC with the Pd/MWCNT catalyst as the anode and proved that during the fuel cell practical operation, ethanol was selectively oxidized to acetic acid on the Pd catalyst in alkaline media.

5 Oxygen reduction electrocatalysis

Cathode performance in alkaline media is generally higher than that in acid media. The improved performance can be attributed to both the inherently faster kinetics of the ORR and the lower degree of the spectator species, including H_{upd}, OH_{ads}, HSO_4, Cl_{ads}, and Br_{ads}, adsorbed onto the electrode surface in alkaline media [110–112]. The ORR in alkaline media proceeds through the four-electron pathway or two-electron pathway [113]. The four-electron pathway can be further divided into the direct pathway, as indicated in Eq. 2, and the series pathway, i.e.,

$$O_2 + H_2O + 2e^- \rightarrow HO_2^- + OH^- \quad (8)$$

and

$$HO_2^- + H_2O + 2e^- \rightarrow 3OH^- \quad (9)$$

The difference is that for the former, oxygen proceeds directly to OH^- as the final product through a four-electron transfer, whereas for the latter, OH_2^- is first given as an intermediate by a two-electron process and then subsequently reduced to OH^-. With regard to the two-electron pathway, the intermediate OH_2^- in Eq. (5) will decompose into O_2 and OH^-, i.e.,

$$2HO_2^- \rightarrow 2OH^- + O_2 \quad (10)$$

Thus far, a variety of materials have been investigated for the ORR in alkaline media, including Pt group metals-based catalysts [114–116], Ag-based catalysts [117–119], manganese oxide catalysts [120–122], perovskite catalysts [123–125], spinels oxide catalysts [126–128], and macrocycle catalysts [129–131]. Carbon support has also been noted to show catalytic activity toward the ORR in alkaline media through the two-electron pathway [132]. Among all pure metals, the Pt catalyst shows the highest catalytic activity toward the ORR in alkaline media. Ag is a promising replacement of Pt for the ORR in alkaline media because it has a comparable activity, much lower cost, higher stability, and is more tolerant to alcohol than Pt [133–138]. In the following, we focus on the discussion of Ag-based cathode catalysts for ORR in alkaline media. The mechanism of the ORR on Ag-based catalysts in alkaline media is similar to that on Pt, which can proceed with the primary four-electron pathway [111,112]. Blizanac et al. investigated the ORR on Ag low-index single crystals in alkaline media in the temperature range of 293–333 K. The rotating ring disk testing results showed that the ORR proceeded as an entirely four-electron reduction with very small peroxide formation (0.5%–2%) in the testing temperature range and that the kinetics of the ORR was structure-sensitive and increased in the order (100)$\leqslant$(111)$\leqslant$(110). Coutanceau et al. [118,134] compared ORR activity in alkaline media on both Pt/C and Ag/C catalysts with a 20 wt% metal loading; a larger overpotential of 50 mV was observed on the Ag/C catalyst compared with that on the Pt/C catalyst in an alkali concentration of 0.1 M NaOH. However, in the presence of methanol, the Ag catalyst displayed better tolerance toward methanol than did the Pt/C catalyst when the methanol concentration was higher than 0.1 M. Chatenet et al. [135] studied the influences of both temperature and sodium hydroxide concentration on the ORR activity on Ag/C and Pt/C catalysts, and demonstrated that a temperature increase favored the ORR activity on both metals, whereas an alkali concentration increase was only positive for the ORR on the Ag/C catalyst. The ORR on the Pt/C catalyst was hindered by the alkali concentration increase, which could be attributed to greater adsorbed species coverage on Pt. Furuya et al. [136] examined the long-term stability of oxygen cathode loaded with Pt and Ag catalysts and found that the cathode loaded with the Ag catalyst showed a longer lifetime of three years, whereas it was only one year for that with the Pt catalyst under the practical chlor-alkali electrolysis condition. Modification of the Ag catalyst with a higher performance has been studied by different groups [139–141]. Lee et al. [139] synthesized bimetallic AgMg catalysts, and the highest current density was obtained with an Ag/Mg atomic ratio of 3. Lima et al. [140] investigated ORR on carbon supported AgCo bimetallic catalysts in alkaline media; the results suggested that AgCo/C catalysts showed higher activity for the ORR than Pt/C, which could be ascribed to a stronger interaction of oxygen with the Ag atoms, thus facilitating the O-O bond splitting and increasing the ORR kinetics. Tungsten carbide nanocrys-

tals promoting Ag catalyst was prepared by Shen et al. [141] and was investigated as the electro-catalyst for the ORR in alkaline media. The results demonstrated that the addition of W_2C to Ag/C could reduce the overpotential of the ORR on the Ag/C catalyst in alkaline media significantly. The W_2C-Ag/C catalyst showed a high and unique activity toward the ORR, which was similar to that of Pt and an immunity to alcohol oxidation. Thus far, the Ag-based catalysts studied for the ORR in alkaline media still possess relatively larger particle size (7–500 nm) [118, 119,129,135]. Hence, to obtain the high performance of the ORR in alkaline media, developing new methods to obtain highly dispersed and much smaller Ag nanoparticles is imperative.

In summary, under alkaline conditions, the kinetics of both EOR and ORR become more facile than in acidic media, making it possible to use non-platinum catalysts. This section summarizes the recent studies of non-platinum electro-catalysts for EOR and ORR in alkaline media. The discussion has been focused on two types of electro-catalyst, Pd-based catalysts for EOR and Ag-based catalysts for ORR. In the case of Pd-based catalysts for EOR in alkaline media, ethanol is oxidized selectively to acetic acid, rather than the final product of CO_2. In the case of Ag-based catalysts for ORR in alkaline media, Ag-based catalysts present a larger particle size than Pt-based catalysts. The catalytic activity, durability, and utilization of Pd- and Ag-based catalysts need to be enhanced further.

6 Single cell design and performance

The preceding review indicates that both the ionic conductivity of anion-exchange membranes and the catalytic activity of anode catalysts are still low. The applications of the state-of-the-art membranes and catalysts to the AEM DEFC setup described in Section 2 and shown in Fig. 1 still cannot result in a satisfactory performance. An effective approach to increase the kinetics of both EOR and ORR and enhance the ionic conductivity of the membrane is to add an alkali (typically the KOH) to the fuel solution [65,89,109,142–145]. A number of works that used A201 membranes with added alkaline ethanol solutions have been reported [89, 109, 142–144]. Fujiwara et al. [143] compared cell performance between acid- (using the Nafion-117 membrane) and alkaline-based (using A201 membrane) DEFCs with unsupported PtRu and Pt as the anode and cathode catalysts, respectively. The results are presented in Fig. 6, which also shows that the peak power density of the AEM DEFC increases from 6 to 58 mW/cm^2 at room temperature and atmospheric pressure with humidified oxygen of 100 sccm when the acid membrane is changed to an alkaline one. The main product of the EOR in the AEM DEFC was found to be acetic acid, whereas both acetaldehyde and acetic acid were detected in the 1 : 1 ratio

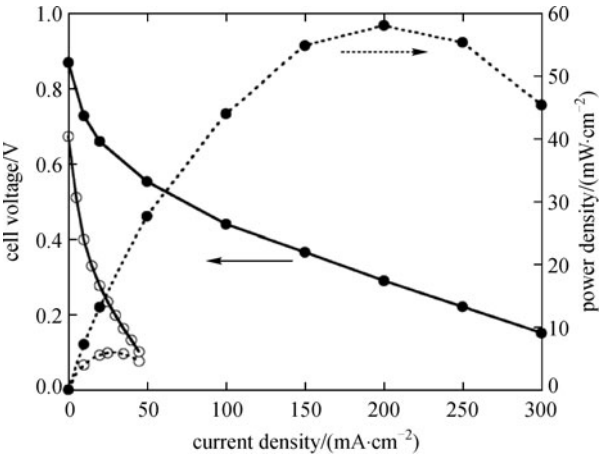

Fig. 6 Cell performance of an AEM DEFC using an AEM and 1.0 M ethanol + 0.5 M KOH solution (•) or a CEM and 1.0 M ethanol aqueous solution (○) (4 mL/min), as an electrolyte membrane and fuel, respectively, at room temperature and atmospheric pressure. Anode: 3 mg/cm^2 PtRu black, cathode: 3 mg/cm^2 Pt black, and cathode gas: humidified O_2 (100 mL/min) [143]

in the PEM DEFC. This fact suggests that the Faradic efficiency of the EOR in the AEM DEFC is higher than that in the PEM DEFC. Hence, the AEM DEFC is superior to the PEM DEFC. In alkaline media, the kinetics of the EOR on Pd-based catalysts has been found to be higher than that on Pt-based catalysts [19]. For this reason, many cell performance tests have focused on the use of Pd-based catalysts [89,109,144]. Bianchini et al. [109] tested a passive AEM DEFC with an A201 membrane at room temperature, Pd/MWCNT as the anode catalyst, and Fe-Co Hypermec^{TM} K14 as the cathode catalyst. The results of their test showed that when the cell was fed with 2.0 M KOH and 10% (mass fraction) ethanol, the OCV was as high as 0.74 V and the peak power density was 18.4 mW/cm^2. When the same cell setup was used but the passive operation was changed to the active supply of reactants, the peak power density of the active AEM DEFC reached 52 and 74 mW/cm^2 at 60°C and 80°C, respectively. Zhao et al. [89] compared the cell performance of active AEM DEFCs with an oxygen flow rate of 100 sccm and made up of Pd/C and PdNi/C as the anode catalysts, Fe-Co Hypermec^{TM} K14 as the cathode catalyst, and A201 membrane as the alkaline conducting membrane. The results shown in Fig. 7 indicate that the PdNi/C anode catalyst caused the OCV to reach as high as 0.89 V and the peak power density to high as 90 mW/cm^2 at 60°C. In the case of Pd/C, the OCV was 0.79 V, and the peak power density was 67 mW/cm^2 at the same temperature. Bianchini et al. [144] synthesized the Pd-(Ni-Zn)/C anode catalyst with selective oxidation of ethanol to acetic acid. Using the same cathode, membrane, and operating conditions as those in the reference [109], the passive AEM DEFC at room temperature could yield a power density of as high as 55 mW/cm^2, whereas the active

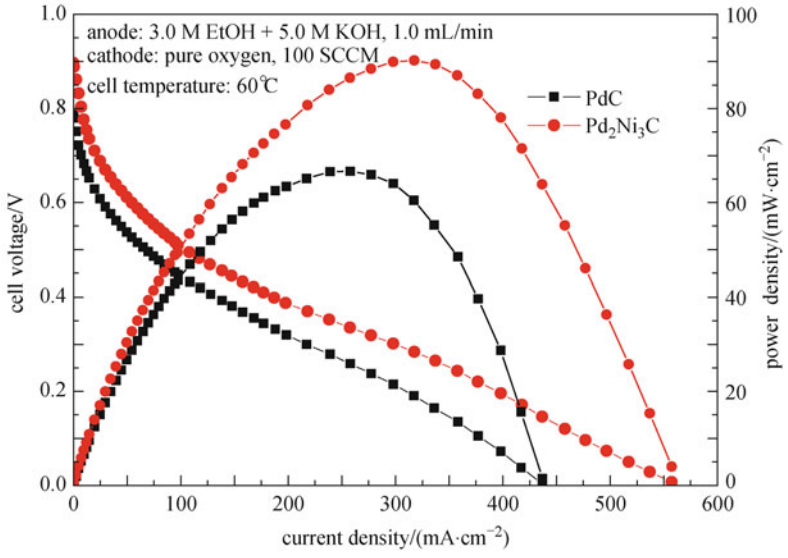

Fig. 7 Cell performance of an AEM DEFC with different anode catalysts [89]

AEM DEFC delivered up to 160 mW/cm^2 with an oxygen flow rate of 200 sccm at 80°C, as shown in Fig. 8, representing the highest performance of AEM DEFCs that has so far been reported in open literature. Note that the highest performance reported in active PEM DEFCs with the PtSn/C as the anode, Nafion-115 as the PEM, and Pt/C as the cathode is only 79.5 mW/cm^2 with oxygen pressure of 0.2 MPa at 90°C [145]. Cell performance based on the alkali-doped PBI membrane has also been studied [65, 146]. Sun et al. [65] tested the active AEM DEFC with PtRu/C anode and Pt/C cathode, and the oxygen at 0.2 MPa was supplied to the cathode. The results indicated that the peak power densities at 75 and 80°C were 49.20 and 60.95 mW/cm^2, respectively. Modestov et al. [146] reported the performance of the air-breading AEM DEFC using RuV/C anode and TMPhP/C cathode, and the peak power density of was 100 mW/cm^2 at 80°C.

Li et al. [142] studied the effect of the operating conditions on the cell performance, including cell operating temperature and concentrations of both ethanol and KOH. The results showed that the peak power density was 12 mW/cm^2 at 30°C, and it almost tripled to 30 mW/cm^2 at 60°C. However, there was an optimal ethanol concentration under which the fuel cell had the best cell performance. In addition, the cell performance increased monotonically with increasing KOH concentration in the low current densities, whereas in the high current densities, there was an optimal KOH concentration in terms of cell performance. The effect of the content of two types of polymer binder (i.e., A3-an anion-conducting ionomer developed by Tokuyama and PTFE-a neutral polymer) in the anode CL on cell performance was also evaluated by Zhao et al. [147]. Their results indicated that in the case of feeding C_2H_5OH-KOH solution, as shown in Fig. 9, cell performance decreased with the increase in the A3 content. However, in the case of feeding C_2H_5OH solution without

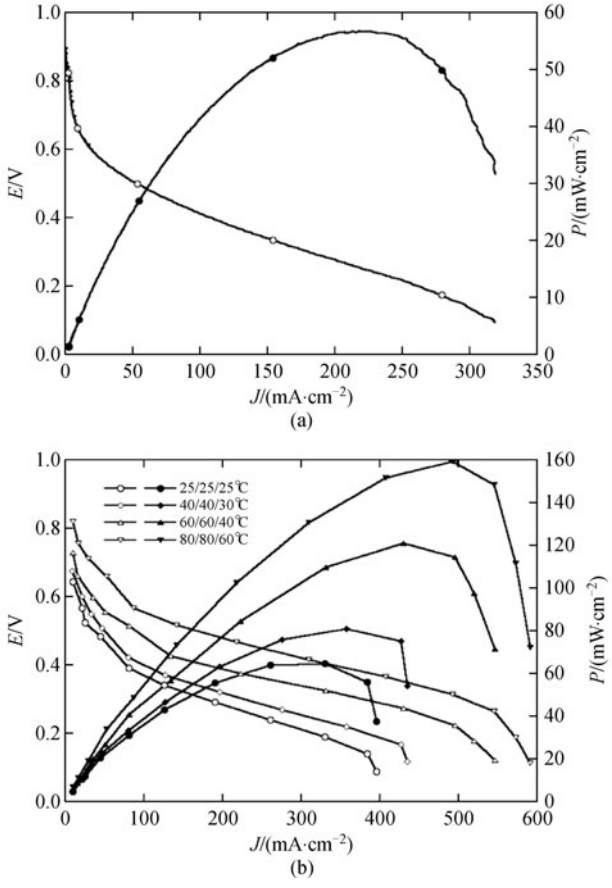

Fig. 8 Cell performance of an AEM DEFC fuelled with a 2 M KOH solution of ethanol (10%): (a) air-breathing system at 20°C and (b) active system, 4 mL/min EtOH, O_2 flow 200 mL/min. In either case, the MEA (5 cm^{-2}) was composed of a Pd-(Ni-Zn)/C anode (Ni foam), Hypermec^{TM} K-14 Fe-Co cathode (carbon cloth), and Tokuyama A006 membrane. Pd loading 1 mg/cm^2. The inset of b presents the temperature of fuel (left), cell (central) and oxygen gas (right) [144]

adding KOH, cell performance varied with the A3 ionomer content in the anode CL as shown in Fig. 10. The content of 10% (mass fraction) exhibited the best performance. Ogumi et al. [148] proposed a novel approach that used a positively charged inorganic compound, a layered double hydroxide (LDH), as an anion conductor in AEM-based fuel cells in the case where KOH was added in the solution to improve the triple-phase boundaries of CLs. In addition, Zhao et al. [149] recently reported that cathode flooding occurred in an AEM DEFC that significantly affected the cell performance, primarily because the diffusion flux from the anode to cathode outweighed the total water flux due to both oxygen reduction reaction and EOD. More interestingly, rather than in acid electrolyte-based fuel cells where cathode flooding occurred at a high (limiting) current, in an AEM DEFC, cathode flooding occurred at an intermediate current.

In summary, the cell performance of AEM DEFC with different catalyst materials, structures, and operating conditions has been discussed. The DEFC with the Pd-(Ni-Zn)/C anode catalysts, A201 AEM membrane, and Fe-Co Hypermec^{TM} K14 cathode catalysts based on the KOH mixed ethanol solution shows the best cell performance. To enhance cell performance further, significant research should also be conducted in the aspects of understanding species transport mechanisms and designing new electrode structures.

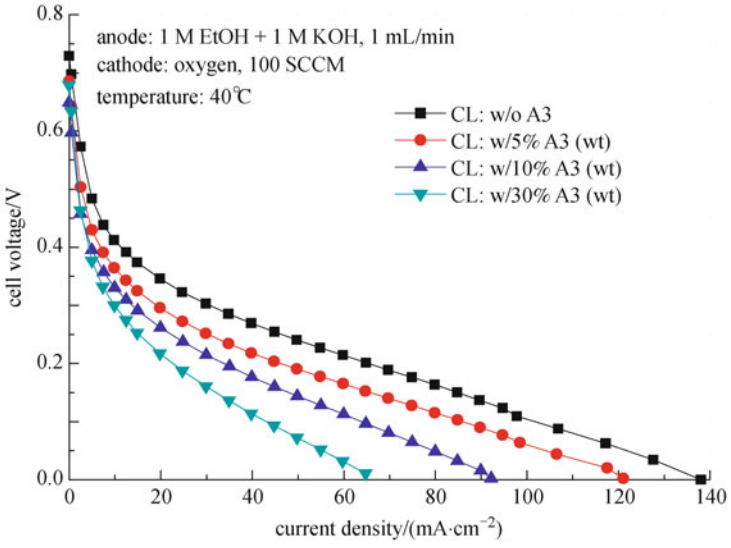

Fig. 9 Effects of the A3 content in the anode catalyst layer on cell performance in the case with KOH in the ethanol solution [147]

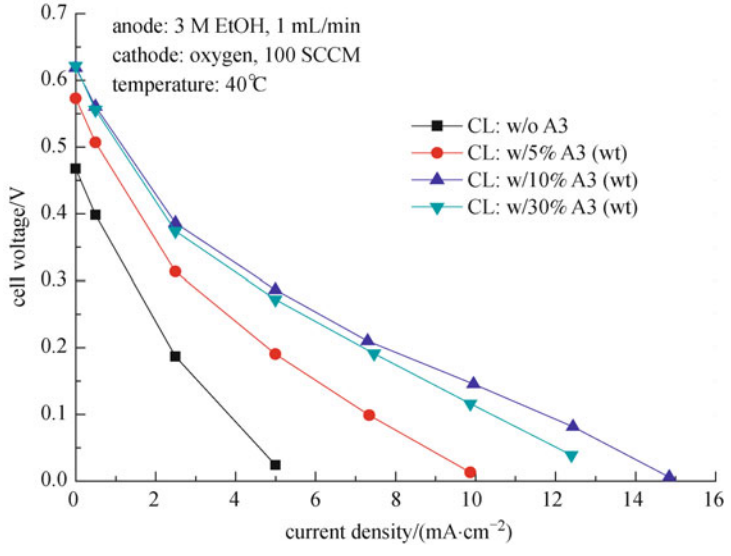

Fig. 10 Effects of the A3 content in the anode catalyst layer on cell performance in the case without KOH in the ethanol solution [147]

7 Summary and outlook

Ethanol is a sustainable, carbon-neutral transportation fuel source. It is an ideal fuel source for direct oxidation fuel cells for portable and mobile applications because it offers multiple advantages over hydrogen and methanol, including higher energy density and ease of transportation, storage, and handling. However, conventional DEFCs that use Nafion membranes and platinum-based catalysts exhibit extremely low performance (the highest peak power density reported thus far is 79.5 mW/cm^2 at 90°C). This article presents a review of the current status of a relatively new type of DEFC that uses anion-exchange membranes and non-platinum catalysts. This AEM DEFC with PdNi/C anode catalyst, FeCo/C cathode catalyst, and KOH mixed ethanol solution has been shown to yield a much better performance at the highest peak power density of 160 mW/cm^2 at 80°C. Aside from this encouraging cell performance, this type of AEM DEFC offers the advantage of low cost resulting from relatively cheaper membranes and non-platinum catalysts compared with those in acid membrane-based fuel cells. However, the power output of the AEM DEFC must be substantially improved before widespread commercialization is possible. Such improvement depends on finding solutions to many critical issues. The most important and most challenging issue is achieving a direct 12-electron electro-oxidation of ethanol to CO_2 and water. Moreover, a significant improvement is needed to upgrade OH^- conductivity and thermal stability of existing membranes. The electrode design must be optimized, which critically depends on a clear understanding of mass/charge transport in nanosized electrode structures. The following are some of the critical issues that need to be addressed in the future:

1) Membranes: Aside from the abovementioned challenging issue of developing an anion-exchange membrane with both high ionic conductivity and high stability, research should be done with regard to the aspects of characterizations of anion-exchange membrane properties, including water uptake, ethanol permeability, water diffusivity, and electro-osmotic drag coefficient.

2) Ionomers: An ionomer is essential to bind discrete catalyst particles and form a porous CL that facilitates the transfer of ions, electrons, and reactants/products simultaneously. However, similar to the anion-exchange membrane, both the ionic conductivity and thermal and chemical stability of the present ionomers are still low. Hence, significant work is needed to enhance ionic conductivity and stability of ionomers. An ionomer that can dissolve in a nontoxic solvent is also required.

3) Anode catalysts: Pd-based catalysts show appreciable performance toward the EOR in alkaline media. Nevertheless, both the activity and durability of Pd catalyst for the EOR in alkaline media need to be enhanced further, and the design of multi-metallic electro-catalysts is essential. Presently, ethanol oxidation on the Pd catalyst is incomplete and is oxidized selectively to acetic acid. The development of highly active anode catalysts for ethanol oxidation to CO_2 is required because it will increase the Faradic efficiency of the EOR.

4) Cathode catalysts: The kinetics of the ORR in alkaline media is faster than in acidic media, making it possible to use non-platinum metal catalysts. A challenging issue in the cathode material is how to enhance the catalytic activity of non-Pt catalysts and make them comparable with that of Pt. So far, the Ag-based cathode catalyst for the ORR in alkaline media still presents a larger particle size (7–500 nm) than do Pt-based catalysts. Hence, another target in the cathode material is the development of new synthesis methods that can lead to high electrochemical surface area Ag-based catalysts.

5) Water transport: Water is produced at the anode and consumed at the cathode. A high water crossover from the anode to cathode can increase water uptake of the membrane, thereby improving ionic conductivity. However, it also tends to increase possible cathode flooding, leading to an increase in oxygen transport resistance. In contrast, a low water crossover can facilitate oxygen transport, but it also tends to increase mass transport loss for the ORR, resulting in a high cathode activation loss. Hence, the management of the water transport is another key issue.

6) Ethanol transport: Maintaining the right ethanol concentration level in the anode CL is critically important. A too high ethanol concentration in the anode CL will cause two problems: 1) the reduction of the coverage of hydroxide ions in the CL that can increase anode activation loss and 2) the increase of ethanol crossover that can reduce fuel utilization. Note that in AEM DEFCs, because the cathode catalyst (non-Pt) is generally tolerant to ethanol oxidation, the mixed potential problem as a result of fuel crossover is not as serious as in PEM DMFCs. However, a too low ethanol concentration level in the anode CL will increase mass transport loss and reduce the limiting current. It should be understood that the ethanol concentration in the anode CL is affected by the design of the anode flow field and anode DL as well as by operating conditions, including the ethanol concentration supplied to the flow field and the ethanol solution flow rate in the flow field.

7) CO_2: When air is used as the oxidant, CO_2 from the air [CO_2 concentration in the air is around 0.039% (volume fraction) under standard conditions] can react with the OH^- generated by the ORR to form CO_3^{2-}. The formation of CO_3^{2-} may affect cell performance in two aspects: 1) by decreasing the pH level in the cathode CL, thus affecting the kinetic of the ORR and 2) by reducing the ionic conductivity in both the cathode CL and membrane, increasing cell resistance. Hence, the problem associated with CO_2 from air is an issue that needs to be addressed in the future.

8) KOH: KOH that penetrates through the membrane from the anode to cathode can react with CO_2 to form carbonation precipitation that blocks the pores of both membrane and electrode, lowering the active surface area and hindering species transport. The presence of KOH in the cathode can also reduce the hydrophobicity of the gas diffusion layer, thereby breaking the balance of mass transport between water and oxygen. Hence, the alleviation or elimination of the KOH crossover is a key issue. In addition, the effects of the added alkali on the anion exchange membrane and catalysts during a long operation also need to be addressed.

Acknowledgements This work was supported by a grant from the Research Grants Council of the Hong Kong Special Administrative Region, China (Project No. 623709).

T.S. Zhao is a Professor of Mechanical Engineering and the Director of Center for Sustainable Energy Technology at the Hong Kong University of Science & Technology (HKSUT). As an internationally renowned expert in energy technology, he presently focuses his research on fuel cells, multi-scale multiphase heat/mass transport with electrochemical reactions, and computational modeling. As of October 2010, he has published more than 150 papers in prestigious journals in the fields of energy science and engineering with SCI citations of more than 2850 times and H-index of 30. He has received a number of recognitions for his research and teaching, including the Bechtel Foundation Engineering Teaching Excellence Award at HKUST in 2004, the Overseas Distinguished Young Scholars Award by National Natural Science Foundation of China in 2006, Fellow of the American Society of Mechanical Engineers (ASME) in 2007, the Croucher Senior Fellowship award from the Croucher Foundation in 2008, and the Yangtze River Chair Professorship by the Chinese Ministry of Education in 2010. In the international community, Prof. Zhao serves as Editor-in-Chief of *Advances in Fuel Cells*, Series Editor, *Energy & Environment* (Royal Society of Chemistry), Asian Regional Editor of *Applied Thermal Engineering*, and as a member of the Editorial Board for more than 18 International Journals.

References

1. Prakash S, Kohl P A J. Performance of carbon dioxide vent for direct methanol fuel cells. Power Sources, 2009, 192(2): 429–434
2. Song S Q, Tsiakaras P. Recent progress in direct ethanol proton exchange membrane fuel cells (DE-PEMFCs). Appl Catal. B: Environ, 2006, 63(3,4): 187–193
3. Tu H C, Wang Y Y, Wan C C, Hsueh K L. Semi-empirical model to elucidate the effect of methanol crossover on direct methanol fuel cell. J Power Sources, 2006, 159(2): 1105–1114
4. Schultz T, Krewer U, Vidakovic T, Pfafferodt M, Christov M, Sundmacher K. Systematic analysis of the direct methanol fuel cell. J. Appl Electrochem, 2007, 37(1): 111–119
5. Scott K, Taama W M, Argyropoulos P, Sundmacher K. The impact of mass transport and methanol crossover on the direct methanol fuel cell. J Power Sources, 1999, 83(1,2): 204–216
6. Chetty R, Kundu S, Xia W, Bron M, Schuhmann W, Chirila V, Brandl W, Reinecke T, Muhler M. PtRu nanoparticles supported on nitrogen-doped multiwalled carbon nanotubes as catalyst for methanol electrooxidation. Electrochimi Acta, 2009, 54(17): 4208–4215
7. Zhao H B, Yang J, Li L, Li H, Wang J L, Zhang Y M. Effect of over-oxidation treatment of Pt-Co/polypyrrole-carbon nanotube catalysts on methanol oxidation. Int J Hydrogen Energy, 2009, 34 (9): 3908–3914
8. Song Y J, Han S B, Lee J M, Park K W. PtRu alloy nanostructure electrodes for methanol electrooxidation. J Alloy Compd, 2009, 473(1,2): 516–520
9. Han J H, Liu H T. Real time measurements of methanol crossover in a DMFC. J Power Sources, 2007, 164(1): 166–173
10. Heinzel A, Barragan V M. A review of the state-of-the-art of the methanol crossover in direct methanol fuel cells. J Power Sources, 1999, 84(1): 70–74
11. Ren X, Springer T E, Gottesfeld S. Water and Methanol uptakes in nafion membranes and membrane effects on direct methanol cell performance. J Electrochem Soc, 2000, 147(1): 92–98
12. Antolini E. Catalysts for direct ethanol fuel cells. J Power Sources, 2007, 170(1): 1–12
13. Fujiwara N, Friedrich K A, Stimming U. Ethanol oxidation on PtRu electrodes studied by differential electrochemical mass spectrometry. J Electroanal Chem, 1999, 472(2): 120–125
14. Pramanik H, Wragg A A, Basu S. Studies on operating parameters and cyclic voltammetry of a direct ethanol fuel cell. J Appl Electrochem, 2008, 38(9): 1321–1328
15. Zhou W J, Li W Z, Song S Q, Zhou Z H, Jiang L H, Sun G Q, Xin Q, Poulianitis K, Kontou S, Tsiakaras P. Bi- and tri-metallic Pt-based anode catalysts for direct ethanol fuel cells. J Power Sources, 2004, 131(1,2): 217–223
16. Song S Q, Zhou W J, Zhou Z H, Jiang L H, Sun G Q, Xin Q, Leonditis V, Kontou S, Tsiakaras P. Pt-based catalysts for direct ethanol fuel cells Int J Hydrogen Energy, 2005, 30(9) : 995–1001
17. Colmenares L, Wang H, Yusys Z, Jiang L, Yan S, Sun G Q, Behm R J. Ethanol oxidation on novel, carbon supported Pt alloy catalysts—Model studies under defined diffusion conditions. Electrochim Acta, 2006, 52(1): 221–233
18. Lamy C, Rousseau S, Belgsir E M, Coutanceau C, Léger J M, Recent progress in the direct ethanol fuel cell: development of new platinum-tin electrocatalysts. Electrochim Acta, 2004, 49(22,23): 3901–3908
19. Bianchini C, Shen P K. Palladium-based electrocatalysts for alcohol oxidation in half cells and in direct alcohol fuel cells. Chem Rev, 2009, 109(9): 4183–4206
20. Antolini E, Gonzalez E R. Alkaline direct alcohol fuel cells, J Power Sources, 2010, 195(11): 3431–3450
21. Varcoe J R, Slade R C T. Prospects for alkaline anion-exchange membranes in low temperature fuel cells. Fuel Cells, 2005, 5(2): 187–200
22. Yu E H, Scott K, Reeve R W. electrochemical reduction of oxygen on carbon supported pt and pt/ru fuel cell electrodes in alkaline

solutions. Fuel Cells, 2003, 3(4): 169–176
23. Xu J B, Zhao T S, Shen S Y, Li Y S. Stabilization of the palladium ethanol-oxidation electrocatalyst with alloyed gold Int J Hydrogen Energy, 2010, 35(13): 6490–6500
24. Rao V, Hariyanto, Cremers C, Stimming U. Investigation of the ethanol electro-oxidation in alkaline membrane electrode assembly by differential electrochemical mass spectrometry. Fuel Cells, 2007, 7(5): 417–423
25. Varcoe J R, Kizewski J P, Halepoto D M, Poynton S D, Slade R C T, Zhao F. Anion-Exchange Membranes. Encyclopedia of Electrochemical Power Sources, Amsterdam, 2009, 329–343
26. Wang Y, Li L, Hu L, Zhuang L, Lu J T, Xu B Q. A feasibility analysis for alkaline membrane direct methanol fuel cell: thermodynamic disadvantages versus kinetic advantages. Electrochem Commun, 2003, 5(8): 662–666
27. Yanagi H, Fukuta K. Anion Exchange Membrane and Ionomer for Alkaline Membrane Fuel Cells (AMFCs). ECS Trans, 2008, 16(2): 257–262
28. Agel E, Bouet J, Fauvarque J F. Characterization and use of anionic membranes for alkaline fuel cells. J Power Sources, 2001, 101(2): 267–274
29. Wan Y, Peppley B, Creber K A M, Bui V T, Halliop E. Quaternized-chitosan membranes for possible applications in alkaline fuel cells. J Power Sources, 2008, 185(1): 183–187
30. Xu T W, Liu Z M, Li Y, Yang W H. Preparation and characterization of Type II anion exchange membranes from poly (2,6-dimethyl-1,4-phenylene oxide) (PPO). J Membr Sci, 2008, 320(1,2): 232–239
31. Pandey A K, Goswami A, Sen D, Mazumder S, Childs R F. Formation and characterization of highly crosslinked anion-exchange membranes. J Membr Sci, 2003, 217(1,2): 117–130
32. Slade R C T, Varcoe J R. Investigations of conductivity in FEP-based radiation-grafted alkaline anion-exchange membranes. Solid State Ionics, 2005, 176(5,6): 585–597
33. Varcoe J R, Slade R C T, Yee E L H, Poynton S D, Driscoll D J, Apperley D C. Poly(ethylene-*co*-tetrafluoroethylene)-derived radiation-grafted anion-exchange membrane with properties specifically tailored for application in metal-cation-free alkaline polymer electrolyte fuel cells. Chem Mater, 2007, 19(10): 2686–2693
34. Varcoe J R, Slade R C T. An electron-beam-grafted ETFE alkaline anion-exchange membrane in metal-cation-free solid-state alkaline fuel cells. Electrochem Commun, 2006, 8(5): 839–843
35. Grew K N, Chu D, Chiu W K S. Ionic equilibrium and transport in the alkaline anion exchange membrane. J. Electrochem Soc, 2010, 157(8): B1024–B1032
36. Wan Y, Peppley B, Creber K A M, Bui V T. Anion-exchange membranes composed of quaternized-chitosan derivatives for alkaline fuel cells J Power Sources, 2010, 195(12): 3785–3793
37. Lu S F, Pan J, Huang A B, Zhuang L, Lu J T. Alkaline polymer electrolyte fuel cells completely free from noble metal catalysts. PNAS, 2008, 105(52): 20611–20614
38. Hibbs M R, Fujimoto C H, Cornelius C J. Synthesis and characterization of poly(phenylene)-based anion exchange membranes for alkaline fuel cells. Macromolecules, 2009, 42(21): 8316–8321
39. Wang G G, Weng Y M, Chu D, Xie D, Chen R R. Preparation of alkaline anion exchange membranes based on functional poly(ether-imide) polymers for potential fuel cell applications. J Membr Sci, 2009, 326(1): 4–8
40. Xiong Y, Liu Q L, Zhang Q G, Zhu A M. Synthesis and characterization of cross-linked quaternized poly(vinyl alcohol)/chitosan composite anion exchange membranes for fuel cells. J Power Sources, 2008, 183(2): 447–453
41. Wang E D, Zhao T S, Yang W W. Poly (vinyl alcohol)/3-(trimethylammonium) propyl-functionalized silica hybrid membranes for alkaline direct ethanol fuel cells Int J Hydrogen Energy, 2010, 35(5): 2183–2189
42. Wu C M, Wu Y H, Luo J Y, Xu T W, Fu Y X. Anion exchange hybrid membranes from PVA and multi-alkoxy silicon copolymer tailored for diffusion dialysis process. J Membr Sci, 2010, 356 (1,2): 96–104
43. Yang C C, Chiu S J, Lee K T, Chien W C, Lin C T, Huang C A. Study of poly(vinyl alcohol)/titanium oxide composite polymer membranes and their application on alkaline direct alcohol fuel cell. J Power Sources, 2008,184(1): 44–51
44. Lei L, Wang Y X. Quaternized polyethersulfone Cardo anion exchange membranes for direct methanol alkaline fuel cells. J Membr Sci, 2005, 262(1,2): 1–4
45. Salmon E, Guinot S, Godet M, Fauvarque J F. Structural characterization of new poly(ethylene oxide)-based alkaline solid polymer electrolytes. J Appl Polym Sci, 1997, 65(3): 601–607
46. Hou H Y, Sun G Q, He R H, Sun B Y, Jin W, Liu H, Xin Q. Alkali doped polybenzimidazole membrane for alkaline direct methanol fuel cell Int J Hydrogen Energy, 2008, 33(23): 7172–7176
47. Xiong Y, Liu Q L, Zeng Q H. Quaternized cardo polyetherketone anion exchange membrane for direct methanol alkaline fuel cells. J Power Sources, 2009, 193(2): 541–546
48. Stoica D, Ogier L, Akrour L, Alloin F, Fauvarque J F. Anionic membrane based on polyepichlorhydrin matrix for alkaline fuel cell: Synthesis, physical and electrochemical properties. Electrochim Acta, 2007, 53(4): 1596–1603
49. Wu L, Xu T W. Improving anion exchange membranes for DMAFCs by inter-crosslinking CPPO/BPPO blends. J Membr. Sci, 2008, 322(2): 286–292
50. Varcoe J R, Beillard M, Halepoto D M, Kizewski J P, Poynton S D, Slade R C T. Membrane and Electrode Materials for Alkaline Membrane Fuel Cells. ECS Trans, 2008, 16(2): 1819–1834
51. Park J S, Park S H, Yim S D, Yoon Y G, Lee W Y, Kim C S. Performance of solid alkaline fuel cells employing anion-exchange membranes J Power Sources, 2008, 178 (2) 620–626
52. Fukuta K, Inoue H, Watanabe S, Yanagi H. In-situ Observation of CO2 through the Self-purging in Alkaline Membrane Fuel Cell (AMFC). ECS Trans, 2009, 19(31): 23–27
53. Adams L A, Poynton S D, Tamain C, Slade R C T, Varcoe J R. A carbon dioxide tolerant aqueous-electrolyte-free anion-exchange membrane alkaline fuel cell. ChemSusChem, 2008, 1(1,2): 79–81
54. Matsui Y, Saito M, Tasaka A, Inaba M. Influence of carbon dioxide on the performance of anion-exchange membrane fuel cells. ECS Trans, 2010, 25(13) 105–110
55. Einsla B R, Chempath S, Pratt L R, Boncella J M, Rau J, Macomber C, Pivovar B S. Stability of cations for anion exchange

membrane fuel cells. ECS Trans, 2007, 11(1): 1173–1180
56. Xiong Y, Liu Q L, Zhu A M, Huang S M, Zeng Q H. Performance of organic-inorganic hybrid anion-exchange membranes for alkaline direct methanol fuel cells. J Power Sources, 2009, 186(2): 328–333
57. Wu Y H, Wu C M, Li Y, Xu T W, Fu Y X. PVA–silica anion-exchange hybrid membranes prepared through a copolymer crosslinking agent. J Membr Sci, 2010, 350(1,2): 322–332
58. Yang C C, Chiu S J, Chien W C, Chiu S S. Quaternized poly(vinyl alcohol)/alumina composite polymer membranes for alkaline direct methanol fuel cells. J Power Sources, 2010, 195(8): 2212–2219
59. Yang C C. Synthesis and characterization of the cross-linked PVA/TiO_2 composite polymer membrane for alkaline DMFC. J Membr. Sci, 2007, 288(1,2): 51–60
60. Wu Y H, Wu C M, Xu T W, Yu F, Fu Y X. Novel anion-exchange organic–inorganic hybrid membranes: Preparation and characterizations for potential use in fuel cells. J Membr Sci, 2008, 321(2): 299–308
61. Varcoe J R, Slade R C T, Yee E L H, Poynton S D, Driscoll D J. Investigations into the ex situ methanol, ethanol and ethylene glycol permeabilities of alkaline polymer electrolyte membranes. J Power Sources, 2007, 173(1): 194–199
62. Xing B, Savadogo O. Hydrogen/oxygen polymer electrolyte membrane fuel cells (PEMFCs) based on alkaline-doped polybenzimidazole (PBI). Electrochem Commun, 2000, 2(10): 697–702
63. Fu J, Qiao J L, Lv H, Ma J X, Yuan X Z, Wang H J. Alkali doped poly (vinyl alcohol) (PVA) for anion-exchange membrane fuel cells: Ionic conductivity, chemical stability and FT-IR characterizations. ECS Trans, 2010, 25(13): 15–23
64. Leykin A Y, Shkrebko O A, Tarasevich M R. Ethanol crossover through alkali-doped polybenzimidazole membrane. J Membr Sci, 2009, 328(1,2): 86–89
65. Hou H Y, Sun G Q, He R H, Wu Z M, Sun B Y. Alkali doped polybenzimidazole membrane for high performance alkaline direct ethanol fuel cell. J Power Sources, 2008, 182(1): 95–99
66. Varcoe J R. Investigations of the ex situ ionic conductivities at 30°C of metal-cation-free quaternary ammonium alkaline anion-exchange membranes in static atmospheres of different relative humidities. Phys Chem Chem Phys, 2007, 9(12): 1479–1486
67. Li Y S, Zhao T S, Yang W W. Measurements of water uptake and transport properties in anion-exchange membranes. Int J Hydrogen Energy, 2010, 35(11): 5656–5665
68. Stoica D, Alloin F, Marais S, Langevin D, Chappey C, Judeinstein P. Polyepichlorydrine membrane for alkaline fuel cell: Sorption and conduction properties. J Phys Chem B, 2008, 112(39): 12338–12346
69. Abuin G C, Nonjola P, Franceschini E A, Izraelevitch F H, Mathe M K, Corti H R. Characterization of an anionic-exchange membranes for direct methanol alkaline fuel cells Int J Hydrogen Energy, 2010, 35(11): 5849–5854
70. Zawodzinski T A, Springer T E, Davey J, Jestel R, Lopez C, Valerio J, Gottesfeld S. A comparative study of water uptake by and transport through ionomeric fuel cell membranes. J Electrochem Soc, 1993, 140(7): 1981–1985
71. Choi P, Datta R. Sorption in proton-exchange membranes. J Electrochem Soc, 2003,150(12): E601–E607
72. Colmati F, Antolini E, Gonzalez E R. Effect of temperature on the mechanism of ethanol oxidation on carbon supported Pt, PtRu and Pt_3Sn electrocatalysts. J Power Sources, 2006, 157(1): 98–103
73. Li H Q, Sun G Q, Cao L, Jiang L H, Xin Q. Comparison of different promotion effect of PtRu/C and PtSn/C electrocatalysts for ethanol electro-oxidation. Electrochim Acta, 2007, 52(24): 6622–6629
74. Shen Q M, Min Q H, Shi J J, Jiang L P, Zhang J R, Hou W H, Zhu J J. Morphology-controlled synthesis of palladium nanostructures by sonoelectrochemical method and their application in direct alcohol oxidation. J Phys Chem C, 2009, 113(4): 1267–1273
75. Wang X G, Wang W M, Qi Z, Zhao C C, Ji H, Zhang Z H. High catalytic activity of ultrafine nanoporous palladium for electro-oxidation of methanol, ethanol, and formic acid. Electrochem Commun, 2009, 11(10): 1896–1899
76. Ksar F, Surendran G, Ramos L, Keita B, Nadjo L, Prouzet E, Beaunier P, Hagège A, Audonet F, Remita H. Palladium nanowires synthesized in hexagonal mesophases: application in ethanol electrooxidation. Chem Mater, 2009, 21(8): 1612–1617
77. Xu C W, Shen P K, Liu Y L. Ethanol electrooxidation on Pt/C and Pd/C catalysts promoted with oxide. J Power Sources, 2007,164 (2): 527–531
78. Hu F P, Chen C L, Wang Z Y, Wei G Y. Mechanistic study of ethanol oxidation on Pd-NiO/C electrocatalyst. Electrochim Acta, 2006, 52(3): 1087–1091
79. Chu D B, Wang J, Wang S X, Zha L G, He J G, Hou Y Y, Yan Y G, Lin H S, Tian Z W. High activity of Pd–In_2O_3/CNTs electrocatalyst for electro-oxidation of ethanol. Catal Commun, 2009, 10(6): 955–958
80. He Q G, Chen W, Mukerjee S, Chen S W, Laufek F. Carbon-supported PdM (M = Au and Sn) nanocatalysts for the electrooxidation of ethanol in high pH media. J Power Sources, 2009,187(2): 298–304
81. Zhu L D, Zhao T S, Xu J B, Liang Z X. Preparation and characterization of carbon-supported sub-monolayer palladium decorated gold nanoparticles for the electro-oxidation of ethanol in alkaline media. J Power Sources, 2009, 187(1): 80–84
82. Ksar F, Ramos L, Keita B, Nadjo L, Beaunier P, Remita H. bimetallic palladium – gold nanostructures: application in ethanol oxidation. Chem Mater, 2009, 21(15): 3677–3683
83. Liu Z L, Zhao B, Guo C L, Sun Y J, Xu F G, Yang H B, Li Z. Novel hybrid electrocatalyst with enhanced performance in alkaline media: hollow Au/Pd core/shell nanostructures with a raspberry surface J Phys Chem C, 2009, 113(38): 16766–16711
84. Nguyen S T, Law H M, Nguyen H T, Kristian N, Wang S, Chan S H, Wang X. Enhancement effect of Ag for Pd/C towards the ethanol electro-oxidation in alkaline media. Appl Catal B, 2009, 91 (1,2): 507–515
85. Wang Y, Nguyen T S, Liu X W, Wang X. Novel palladium–lead (Pd–Pb/C) bimetallic catalysts for electrooxidation of ethanol in alkaline media. J Power Sources, 2010, 195(9): 2619–2622
86. Chen Y G, Zhuang L, Lu J T. Non-Pt anode catalysts for alkaline direct alcohol fuel cells. Chin J Catal, 2007, 28(10): 870–874
87. Jou L S, Chang J K, Twhang T J, Sun I W. Electrodeposition of palladium-copper films from 1-ethyl-3-methylimidazolium chloride-tetrafluoroborate ionic liquid on indium tin oxide electrodes. J

Electrochem Soc, 2009,156(6): D193–D197
88. Singh R N, Singh A, Anindita. Electrocatalytic activity of binary and ternary composite films of Pd, MWCNT, and Ni for ethanol electro-oxidation in alkaline solutions. Carbon, 2009, 47(1): 271–278
89. Shen S Y, Zhao T S, Xu J B, Li Y S. Synthesis of PdNi catalysts for the oxidation of ethanol in alkaline direct ethanol fuel cells. J Power Sources, 2010, 195(4): 1001–1006
90. Qiu C C, Shang R, Y F Xie, Bu Y R, Li C Y, Ma H Y. Electrocatalytic activity of bimetallic Pd–Ni thin films towards the oxidation of methanol and ethanol. Mater Chem Phys, 2010, 120 (2,3): 323–330
91. Bambagioni V, Bianchini C, Filippi J, Oberhauser W, Marchionni A, Vizza F, Psaro R, Sordelli L, Foresti M L, Innocenti M. Ethanol oxidation on electrocatalysts obtained by spontaneous deposition of palladium onto nickel-zinc materials. ChemSusChem, 2009, 2 (1): 99–112
92. Zheng H T, Li Y L, Chen S X, Shen P K. Effect of support on the activity of Pd electrocatalyst for ethanol oxidation. J Power Sources, 2006, 163(1): 371–375
93. Xu C W, Chen L Q, Shen P K, Liu Y L. Methanol and ethanol electrooxidation on Pt and Pd supported on carbon microspheres in alkaline media. Electrochem. Commun, 2007, 9(5): 997–1001
94. Yuan D S, Xu C W, Liu Y L, Tan S Z, Wang X, Wei Z D, Shen P K. Synthesis of coin-like hollow carbon and performance as Pd catalyst support for methanol electrooxidation. Electrochem Commun, 2007, 9(10): 2473–2478
95. Hu F P, Shen P K. Ethanol oxidation on hexagonal tungsten carbide single nanocrystal-supported Pd electrocatalyst. J Power Sources, 2007,173(2): 877–881
96. Hu F P, Cui G F, Wei Z D, Shen P K. Improved kinetics of ethanol oxidation on Pd catalysts supported on tungsten carbides/carbon nanotubes Electrochem Commun, 2008, 10(9): 1303–1306
97. Wang Z Y, Hu F P, Shen P K. Carbonized porous anodic alumina as electrocatalyst support for alcohol oxidation. Electrochem Commun, 2006, 8(11): 1764–1768
98. Hu F P, Ding F W, Song S Q, Shen P K. Pd electrocatalyst supported on carbonized TiO_2 nanotube for ethanol oxidation. J Power Sources, 2006, 163(1): 415–419
99. El-Shafei A A, Elhafeez A M, Mostafa H A. Ethanol oxidation at metal–zeolite-modified electrodes in alkaline medium. Part 2: palladium–zeolite-modified graphite electrode. J Solid State Electrochem, 2010, 14(2): 185–190
100. Pandey R K, Lakshminarayanan V. Enhanced electrocatalytic activity of Pd-Dispersed 3,4-polyethylenedioxythiophene film in hydrogen evolution and ethanol electro-oxidation reactions. J Phys Chem C, 2010, 114(18): 8507–8514
101. Pandey R K, Lakshminarayanan V. Electro-oxidation of formic acid, methanol, and ethanol on electrodeposited Pd-polyaniline nanofiber films in acidic and alkaline medium. J Phys Chem C, 2009, 113(52): 21596–21603
102. Su L, Jia W Z, Schempf A, Ding Y, Lei Y. free-standing palladium/polyamide 6 nanofibers for electrooxidation of alcohols in alkaline medium. J Phys Chem C, 2009, 113(36): 16174–16180
103. Zhou W J, Song S Q, Li W Z, Sun G Q, Xin Q, Kontou S, Poulianitis K, Tsiakaras P. Pt-based anode catalysts for direct ethanol fuel cells. Solid State Ionics, 2004, 175(1–4): 797–803
104. Mann J, Yao N, Bocarsly A B. Characterization and analysis of new catalysts for a direct ethanol fuel cell. Langmuir, 2006, 22(25): 10432–10436
105. Liang Z X, Zhao T S, Xu J B, Zhu L D. Mechanism study of the ethanol oxidation reaction on palladium in alkaline media. Electrochim Acta, 2009, 54(8): 2203–2208
106. Cui G F, Song S Q, Shen P K, Kowal A, Bianchini C. First-principles considerations on catalytic activity of Pd toward ethanol oxidation. J Phys Chem C, 2009, 113(35): 15639–15642
107. Fang X, Wang L Q, Shen P K, Cui G F, Bianchini C. An *in situ* Fourier transform infrared spectroelectrochemical study on ethanol electrooxidation on Pd in alkaline solution. J Power Sources, 2010, 195(5): 1375–1378
108. Zhou Z Y, Wang Q, Lin J L, Tian N, Sun S G. In situ FTIR spectroscopic studies of electrooxidation of ethanol on Pd electrode in alkaline media. Electrochim Acta, 2010 (in press)
109. Bambagioni V, Bianchini C, Marchionni A, Filippi J, Vizza F, Teddy J, Serp P, Zhiani M. Pd and Pt-Ru anode electrocatalysts supported on multi-walled carbon nanotubes and their use in passive and active direct alcohol fuel cells with an anion-exchange membrane (alcohol = methanol, ethanol, glycerol). J Power Sources, 2009, 190(2): 241–251
110. Markovic N, Gasteiger H. Kinetics of oxygen reduction on Pt(Hkl) electrodes–Implications for the crystallite size effect with supported pt electrocatalysts. J Electrochem Soc, 1997, 144(5): 1591–1597
111. Blizanac B B, Ross P N, Marković N M. Oxygen reduction on silver low-index single-crystal surfaces in alkaline solution: Rotating ring $disk_{Ag(hkl)}$ studies. J Phys Chem B, 2006, 110(10): 4735–4741
112. Blizanac B B, Ross P N, Marković N M. Oxygen electroreduction on Ag(1 1 1): The pH effect. Electrochim Acta, 2007, 52(6): 2264–2271
113. Geniès L, Faure R, Durand R. Electrochemical reduction of oxygen on platinum nanoparticles in alkaline media. Electrochim Acta, 1998, 44(8,9): 1317–1327
114. Xu J B, Zhao T S, Li Y S, Yang W W. Synthesis and characterization of the Au-modified Pd cathode catalyst for alkaline direct ethanol fuel cells. Int J Hydrogen Energy, 2010, 35(18): 9693–9700
115. Xiong L F, Manthiram A. Influence of atomic ordering on the electrocatalytic activity of Pt–Co alloys in alkaline electrolyte and proton exchange membrane fuel cells J Mater Chem, 2004, 14: 1454–1460
116. Demarconnay L, Coutanceau C, Léger J M. Study of the oxygen electroreduction at nanostructured PtBi catalysts in alkaline medium. Electrochim Acta, 2008, 53(8): 3232–3241
117. Gülzow E, Wagner N, Schulze M. preparation of gas diffusion electrodes with silver catalysts for alkaline fuel cells. Fuel Cells, 2003, 3(1,2): 67–72
118. Demarconnay L, Coutanceau C, Léger J M. Electroreduction of dioxygen (ORR) in alkaline medium on Ag/C and Pt/C nanostructured catalysts - effect of the presence of methanol. Electrochim Acta, 2004, 49(25): 4513–4521
119. Guo J S, Hsu A, Chu D, Chen R R. Improving oxygen reduction

reaction activities on carbon-supported Ag nanoparticles in alkaline solutions. J Phys Chem C, 2010, 114(10): 4324–4330
120. Mao L Q, Zhang D, Sotomura T, Nakatsu K. Mechanistic study of the reduction of oxygen in air electrode with manganese oxides as electrocatalysts. Electrochim Acta, 2003, 48(8): 1015–1021
121. Calegaro M L, Lima F H B, Ticianelli E A. Oxygen reduction reaction on nanosized manganese oxide particles dispersed on carbon in alkaline solutions, J Power Sources, 2006,158(1): 735–739
122. Fukuda M, Iida C, Nakayama M. One-step through-mask electrodeposition of a porous structure composed of manganese oxide nanosheets with electrocatalytic activity for oxygen reduction. Mater Res Bull, 2009, 44(6): 1323–1327
123. Hermann V, Dutriat D, Müller S, Comninellis C. Mechanistic Studies of oxygen reduction at La0.6Ca0.4CoO3-activated carbon electrodes in a channel flow cell. Electrochim. Acta, 2000, 46(2,3): 365–372
124. Nissinen T, Valo T, Gasik M, Rantanen J, Lampinen M. Microwave synthesis of catalyst spinel $MnCo_2O_4$ for alkaline fuel cell. J Power Sources, 2002, 106(1,2): 109–115
125. Chang Y M, Wu P W, Eu C Y, Hsieh Y C. Synthesis of $La_{0.6}Ca_{0.4}Co_{0.8}Ir_{0.2}O_3$ perovskite for bi-functional catalysis in an alkaline electrolyte. J Power Sources, 2009, 189(2): 1003–1007
126. Restovic A, Ríos E, Barbato S, Ortiz J, Gautier J L. Oxygen reduction in alkaline medium at thin $Mn_xCo_{3-x}O_4$ ($0 \leqslant x \leqslant 1$) spinel films prepared by spray pyrolysis. Effect of oxide cation composition on the reaction kinetics. J Electroanal Chem, 2002, 522(2): 141–151
127. Koninck M D, Poirier S C, Marsan B. Electrochemical characterization for the oxygen reduction reaction. J Electrochem Soc, 2007, 154(4): A381–A388
128. Ríos E, Abarca S, Daccarett P, Cong H N, Martel D, Marco J F, Gancedo J R, Gautier J L. Electrocatalysis of oxygen reduction on $Cu_xMn_{3-x}O_4$ ($1.0 < x < 1.4$) spinel particles/polypyrrol composite electrodes. Int J Hydrogen Energy, 2008, 33(19): 4945–4954
129. Gojković S L, Gupta S, Savinell R F. Heat-treated iron(III) tetramethoxyphenyl porphyrin chloride supported on high-area carbon as an electrocatalyst for oxygen reduction: Part II. Kinetics of oxygen reduction. J Electroanal Chem, 1999, 462 (1) : 63–72
130. Mocchi C, Trasatti S. Composite electrocatalysts for molecular O_2 reduction in electrochemical power sources. J Mol Catal A, 2003, 204–205: 713–720
131. Tributsch H, Koslowski U I, Dorbandt I. Experimental and theoretical modeling of Fe-, Co-, Cu-, Mn-based electrocatalysts for oxygen reduction. Electrochim Acta, 2008, 53(5): 2198–2209
132. Lima F H B, Ticianelli E A. Oxygen electrocatalysis on ultra-thin porous coating rotating ring/disk platinum and platinum-cobalt electrodes in alkaline media. Electrochim Acta, 2004, 49(24): 4091–4099
133. Lima F H B, Zhang J, Shao M H, Sasaki K, Vukmirovic M B, Ticianelli E A, Adzic R R. Catalytic activity–d-band center correlation for the O_2 reduction reaction on platinum in alkaline solutions. J Phys Chem C, 2007, 111(1): 404–410
134. Coutanceau C, Demarconnay L, Lamy C, Léger J M. Development of electrocatalysts for solid alkaline fuel cell (SAFC). J Power Sources, 2006, 156(1): 14–19
135. Chatenet M, Bultel L G, Aurousseau M, Durand R, Andolfatto F. Oxygen reduction on silver catalysts in solutions containing various concentrations of sodium hydroxide-comparison with platinum. J Appl Electrochem, 2002, 32(10): 1131–1140
136. Furuva N, Aikawa H. Comparative study of oxygen cathodes loaded with Ag and Pt catalysts in chlor-alkali membrane cells. Electrochim Acta, 2000, 45(25,26): 4251–4256
137. Wagner N, Schulze M, Gülzow E. Long term investigations of silver cathodes for alkaline fuel cells. J Power Sources, 2004, 127 (1,2): 264–272
138. Okajima K, Nabekura K, Kondoh T, Sudoh M. Degradation evaluation of gas-diffusion electrodes for oxygen-depolarization in chloralkali membrane cell. J Electrochem Soc, 2005, 152(8): D117–D120
139. Lee H K, Shim J P, Shim M J, Kim S W, Lee J S. Oxygen reduction behavior with silver alloy catalyst in alkaline media. Mater Chem Phys, 1996, 45(3): 238–242
140. Lima F H B, Castro J F R, Ticianelli E A. Silver-cobalt bimetallic particles for oxygen reduction in alkaline media. J Power Sources, 2006, 161(2): 806–812
141. Meng H, Shen P K. Novel Pt-free catalyst for oxygen electroreduction. Electrochem Commun, 2006, 8(4): 588–594
142. Li Y S, Zhao T S, Liang Z X. Performance of alkaline electrolyte-membrane-based direct ethanol fuel cells. J Power Sources, 2009, 187(2): 387–392
143. Fujiwara N, Siroma Z, Yamazaki S, Ioroi T, Senoh H, Yasuda K. Direct ethanol fuel cells using an anion exchange membrane. J Power Sources, 2008, 185(2): 621–626
144. Bianchini C, Bambagioni V, Filippi J, Marchionni A, Vizza F, Bert P, Tampucci A. Selective oxidation of ethanol to acetic acid in highly efficient polymer electrolyte membrane-direct ethanol fuel cells. Electrochem Commun, 2009, 11(5): 1077–1080
145. Jiang L H, Sun G Q, Sun S G, Liu J G, Tang S H, Li H Q, Zhou B, Xin Q. Structure and chemical composition of supported Pt-Sn electrocatalysts for ethanol oxidation. Electrochim Acta, 2005, 50 (27): 5384–5389
146. Modestov A D, Tarasevich M R, Leykin A Y, Filimonov V Y. MEA for alkaline direct ethanol fuel cell with alkali doped PBI membrane and non-platinum electrodes. J Power Sources, 2009, 188(2): 502–506
147. Li Y S, Zhao T S, Liang Z X. Effect of polymer binders in anode catalyst layer on performance of alkaline direct ethanol fuel cells. J Power Sources, 2009, 190(2): 223–229
148. Miyazaki K, Abe T, Nishio K, Nakanishi H, Ogumi Z. Use of layered double hydroxides to improve the triple phase boundary in anion-exchange membrane fuel cells. J Power Sources, 2010, 195 (19): 6500–6503
149. Li Y S, Zhao T S, Chen R. Cathode flooding behaviour in alkaline direct ethanol fuel cells. J Power Sources, 2011, 196(1): 133–139